Wafer-Scale Strain Engineering of Ultrathin Semiconductor Crystalline Layers

Marina S. Leite, Emily C. Warmann, Gregory M. Kimball, Stanley P. Burgos, Dennis M. Callahan, and Harry A. Atwater*

Semiconductor epitaxial alloys are widely used in solid state such as lasers, light-emitting diodes and photovoltaics.[1–3] Currently, the versatility of the semiconductor epitaxial growth required by these applications is restricted today by the limited number of single crystal substrates available in bulk form.[4–7] Moreover, defect-free III-V compound semiconductor alloys are responsible for the widespread application of a vast array of optoelectronic devices including semiconductor lasers, light-emitting diodes, and solar cells. One of the key technological requirements for achieving high quality optoelectronic materials and devices is epitaxial crystal growth.[1] The limit number of single crystal substrates available in bulk form is currently an obstacle to the development of high quality semiconductor heterostructures at a wide variety of compositions and lattice parameters. If one had the option to arbitrarily control substrate lattice parameter in epitaxial growth process, this would enable unprecedented control of strain in compound semiconductor alloys and allow for the development of innovative heterostructures with tunable bandgaps and band offsets for the fabrication of optoelectronic devices with unique characteristics, such as semiconductor lasers,[2] thin film solar cells,[3] photonic crystals,[8] among others.

In a coherent epitaxial growth process, the deposited material assumes the substrate crystal structure and lattice parameter, and the film is free of strain-relieving dislocations. The lattice parameter of the deposited film in the parallel direction ($a_{//}$) is equal to that of the substrate (a_{sub}), and the lattice parameter in the perpendicular direction ($a_{\perp}$) is free to expand or contract due to the existence of traction-free top surface and the Poisson effect, which preserves the material unit cell volume V (**Figure 1**a). For a cubic symmetry, $V = {a_{film}}^3 = a_{\perp} \cdot {a_{//}}^2$, where a_{film} is the lattice parameter of the relaxed film. The lattice mismatch between the film and the substrate induces a tetragonal distortion in the epitaxial film, defined as strain [$\varepsilon = (a_{//} - a_{film})/a_{film}$]. If the film natural lattice parameter a_{film} is smaller (larger) than a_{sub}, it is tensile (compressed) with respect to the substrate and therefore $\varepsilon_{//} > 0$ ($\varepsilon_{//} < 0$). Any material that is lattice-mismatched to the substrate will be strained, causing an increase in the elastic energy of the system. If the elastic energy exceeds the energy associated with introduction of defects such as dislocations, these defects can be introduced into the film to minimize the overall energy. However, the defects compromise the quality of the crystal and therefore device's performance.

Substantial research has been dedicated to develop a defect-free crystalline substrate with tunable lattice parameter that can be used as a template for epitaxial semiconductor growth. Considerable effort has been devoted to the growth of graded layers in order to achieve a final lattice parameter distinct than the one of the substrate initially used.[4–7] However this can lead to dislocations depending on growth conditions and requires additional non-active layers to be grown. Early attempts at synthesis of compliant substrates sought to relieve strain in epitaxial alloys but presented high dislocation densities.[9]

In a different approach, high temperature annealing of a borophosphorosilicate glass compound was used to enable strain relief of Si-Ge epitaxial films by means of elastic strain relief,[10,11] yet film buckling was consistently observed. The high viscosity of the glass used (10^{10} Pa.s at 800 °C) resulted in a time scale for film relaxation larger than the time required for buckling formation in the film. Thus, the strain-relieved film presented a well defined buckling pattern with wavelength of 1 μm. Additionally, heat treatments over 400 °C cannot be performed for III-V semiconductor compound films without plastic deformation of the alloy films. In a separate experiment, relaxation of InGaAs strained regions was achieved in selectively etched mesas that allowed very small areas of the film (300 μm × 300 μm) to relax.[12–14] Although the film relaxes, it is trapped between other mesas, limiting its applicability to device fabrication. Recently, it has been demonstrated that under-cut nanoscale islands allow for InAs film relaxation with 200 nm × 200 nm.[15] However, for photovoltaics and device applications, strain relief over wafer-scale is critical. Alternatively, free-standing elastically-strained nanomembranes were achieved by growing trilayers of $Si/Si_xGe_{1-x}/Si$ and relieving it from the original substrate.[16,17] In these laminate structures, elastic strain is partitioned among layers to achieve elastomechanical equilibrium, and it was shown that this can enable control of silicon band offsets.[18] However these templates consist of a combination of strained layers in a strain-balanced laminate, and thus none of the layers relax to their native lattice parameters.

Dr. M. S. Leite, E. C. Warmann, G. M. Kimball, S. P. Burgos, D. M. Callahan, Prof. H. A. Atwater
Thomas J. Waston Laboratories of Applied Physics
Calfornia Institute of Technology
1200 East Calfornia Blvd., MC 128-95
Pasadena, CA 91125, USA
E-mail: mleite@caltech.edu
Prof. H. A. Atwater
Kavli Nanoscience Institute
California Institute of Technology
1200 East Calfornia Blvd., MC 128-95, Pasadena, CA 91125, USA

DOI: 10.1002/adma.201101309

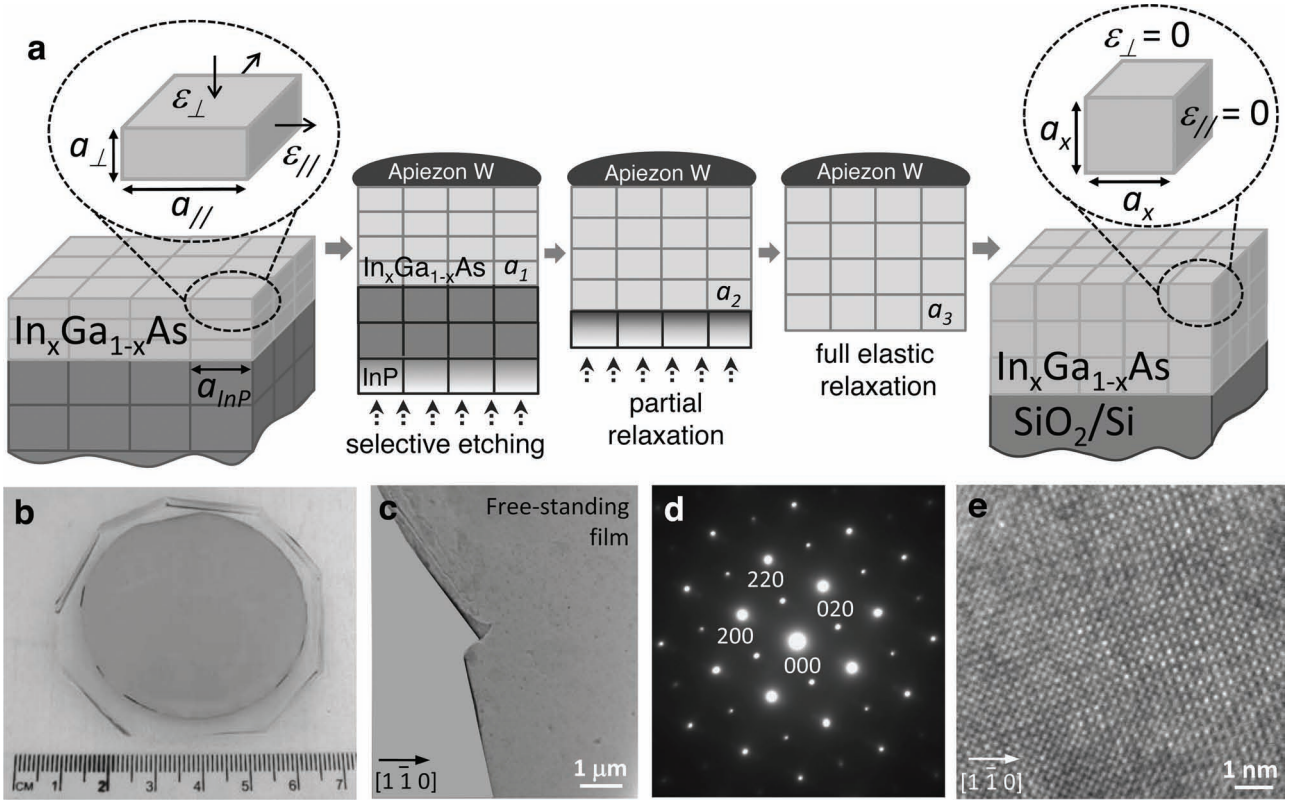

Figure 1. (a) Schematic of heteroepitaxial deposition under biaxial strain and epitaxial template full strain relaxation process. Initially, any in-plane deformation is compensated by an out-of-plane distortion to conserve the unit cell volume. An $In_xGa_{1-x}As$ coherently-strained film can elastically relax through removal of the InP substrate by a selective etching. Apiezon W wax is used as a mechanical support due to its extremely low shear modulus, enabling semiconductor film full relaxation. As a result, the in-plane ($a_{//}$) and out-of-plane ($a_\perp$) lattice parameters of the relaxed film assume the a_x value predicted by Vegard's Law and both $\varepsilon_{//}$ and $\varepsilon_\perp$ are equal to zero. (b) Photograph of a 50 mm diameter $In_{0.43}Ga_{0.57}As$ epitaxial template. (c) Plane view transmission electron microscopy image using g = ⟨220⟩-type diffraction condition of a relaxed free-standing $In_{0.43}Ga_{0.57}As$ film. The absence of dislocations indicates that the relaxed film preserves the original material high quality. (d) Electron diffraction pattern of the region shown in (c). The well defined spots confirm the good crystalline quality of the relaxed film. (e) Atomic resolution plane view transmission electron microscopy image of region shown in (c). The position of the projected atomic columns corresponds to relaxed $In_{0.43}Ga_{0.57}As$.

Successful work has been done using epitaxial lift-off and layer transfer to achieve flexible electronics,[19,20] and to device integration,[21] as well as to decrease the overall cost of a device by substrate reuse.[3,22] Nevertheless, previous reports have largely encompassed the transfer of crystalline layers lattice-matched to the substrate or the use of dislocated sacrificial layers to protect the substrate.

Here we demonstrate the fabrication of a new single crystalline template: 50 mm diameter dislocation-free fully relaxed single crystalline $In_xGa_{1-x}As$ layers with lattice parameter equal to the bulk $In_xGa_{1-x}As$ value. An originally coherently-strained film is distorted in order to match the parallel lattice parameter of the substrate. By removing the substrate, the elastic strain is relieved and the crystal assumes its bulk lattice parameter (Figure 1a). The biaxial in-plane distortion affects the energy bandgap of the alloy, as observed in optical measurements. We have employed a well-known wax compound as a substrate support similar to that used by others. However we also here take advantage of the remarkably high shear relaxation rate of the wax to enable the first wafer-scale single crystalline template. Our demonstration of strain relief in large-area single crystalline layers relies on control of the relative rate of strain relaxation of the semiconductor and wax supporting with an extremely low shear modulus, enabling wafer-scale relief of the excess stress in the semiconductor film. Accordingly, we have characterized here in detail the strain relaxation rate of the wax support, which to our knowledge has never been done. The templates can be used as a building block for epitaxial growth at a variety of lattice parameters, overcoming the limitations to epitaxial growth imposed by existence of only a few available bulk substrates. In particular, epitaxial growth at 5800 Å can enable the fabrication of a monolithic, lattice-matched triple junction solar cell with optimized bandgap, formed by InAlAs (1.92 eV)/InGaAsP (1.42 eV)/InGaAs (0.99 eV). Theoretically, this design can achieve efficiencies hiigher than 50% under 10-suns illumination (concentrated sunlight). The concept demonstrated here can be expanded to other semiconductor alloys.

Our epitaxial template fabrication process begins with 40 nm thick dislocation-free pseudomorphic $In_xGa_{1-x}As$ films with different In content (x), epitaxially grown on InP substrates (Supporting Figure S1). The biaxially-strained $In_xGa_{1-x}As$ films

assume the same parallel lattice parameter of the substrate ($a_{//} = a_{InP}$ and $\varepsilon_{//}$, $\varepsilon_{\perp} \neq 0$). The in-plane strain $\varepsilon_{//}$ between the films and InP ranged from –0.33% to +1.17%, representing both compressive and tensile coherently-strained films (see Supporting Figure S5). The $In_xGa_{1-x}As$ is coated by 2 mm of a thermoplastic wax support,[23,24] to relax and handle the film. Once the film is coated with the wax, the InP is selectively etched, allowing for film relaxation. The $In_xGa_{1-x}As$ is always compressively-strained with respect to the wax, and is thus more stable against crack formation (Figure 1b). The relaxed film is then bonded to a handling substrate,[24] e.g., SiO_2/Si. The wax is removed and the single crystalline template is ready.

The use of the crystalline template as a starting point for epitaxial growth requires one to take into account the existing difference in coefficient of thermal expansion (CTE) between the film and the host substrate. By heating the semiconductor film and the SiO_2/Si system at typical epitaxial growth temperatures (around 600 °C), the bonded film will be slightly compressed along the in-plane direction due to its larger CTE (5.7×10^{-6} °C^{-1} for InGaAs and 0.5×10^{-6} °C^{-1} for SiO_2). However, the integrated stress expected for the 40 nm thick InGaAs film on SiO_2 is approximately 9.6×10^2 dyn·cm^{-1}, which is less than 1% of the value determined to cause relaxation through dislocation introduction at the interface.[25–27]

The fabrication procedure can be scaled up to entire wafers, as illustrated in Figure 1b. The plane view transmission electron microscopy image in Figure 1c shows a free-standing piece of the relaxed $In_xGa_{1-x}As$ film free of cracks or dislocations. The well defined spots of the electron diffraction pattern in Figure 1d confirm that the elastically-relaxed film is a defect-free single crystal. Figure 1e displays an atomic resolution transmission electron microscopy image of a representative region of the template; no defects were observed. Additionally, the distance between the ⟨001⟩ projected atomic columns points out that the lattice parameter is equal to the bulk value. Thus, the overall crystalline quality of the film is preserved upon the methodology presented here (Supporting Figure S1) to achieve elastically-relaxed single crystalline layers.

In order to understand how the strain relief process takes place, rheology measurements were performed using parallel circular plate geometry for a 2 mm thick Apiezon W wax support. The dynamic shear modulus G, which is defined as the deformation of a material when it experiences a force parallel to one of its surfaces while its opposite face experiences an opposing force, can be divided into real and imaginary components, $G = G' + iG''$. The real component expresses energy storage due to in-plane strain, and is defined as the elastic shear modulus. The imaginary component is a measurement of energy dissipation, therefore termed the loss, or viscous shear modulus.[28] According to the measurement shown in **Figure 2**a, the Apiezon W wax is a viscoelastic material, exhibiting both elastic (solid-like) and viscous (liquid-like)

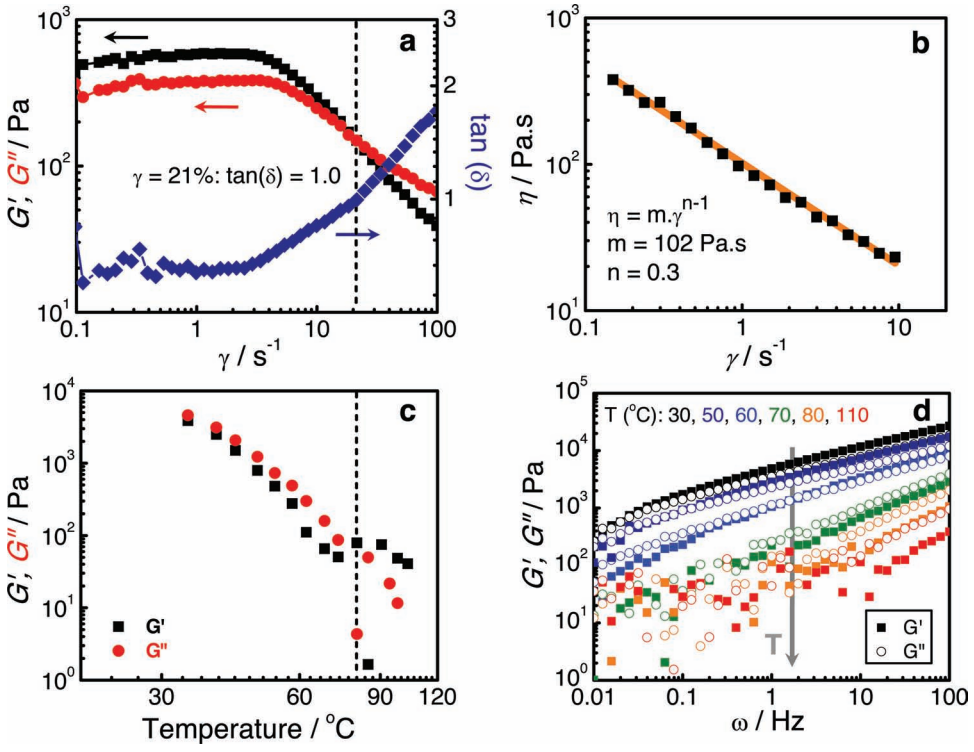

Figure 2. Rheology measurements of the Apiezon W wax. (a) Shear elastic G' and loss G'' moduli as a function of shear rate γ. Right axis show the loss tangent $tan(\delta)$, equal to G''/G'. (b) Viscosity η as a function of rotation plate frequency (temperature was kept constant and equal to 25 °C). (c) G', G'' as a function of temperature for a rotation plate frequency equal to 1 Hz. At 85 °C the wax starts melting and, therefore, its shear modulus decays drastically. (d) Shear moduli G', G'' as a function of rotation plate frequency ω.

properties. At room temperature the wax exhibits a pseudo-plastic flow behavior, with an elastic shear modulus G' equal to 5.8×10^{-7} GPa for $\gamma = 1.0$. The ratio between G' and G'' [or $tan(\delta)$] describes the visco-elastic response of the wax–see Figure 2a. A crossing-point between G' and G'' (at $\gamma = 21\%$) defines the wax transition between an elastic material ($G' > G''$) to a viscous regime ($G' < G''$). Therefore, at a high shear rate γ, which is the velocity of the moving top plate divided by the distance between the plates, the wax behavior is dominantly viscous flow.

The viscosity η of the wax was measured (Figure 2b) and the expected characteristic of non-Newtonian flow behavior were observed, namely a linear decay on a log-log plot as a function of the shear rate γ. A two parameter power law expression (Equation 1) was used to determine the constants characterizing the fluidity of the wax: $m = 102$ Pa·s and $n = 0.3$.

$$\eta = m \cdot \gamma^{n-1} \tag{1}$$

The shear moduli components were measured as a function of temperature T, as illustrated in Figure 2c. At 85 °C the Apiezon W wax starts melting, and its shear moduli decay drastically as a consequence. By increasing the temperature, G'' assumes a larger value than G', consistent with the viscoelastic property of the wax. Figure 2d shows the variation of G' and G'' as a function of the rotation plate frequency ω for various temperatures T. As the wax is heated, its mechanical properties change, as a consequence of molecular weight variations due to solvent evaporation. Note that at 70 °C (green set of data) G'' has a larger value than G', and the wax acts as a viscous fluid. At 80 °C (orange set of data) the wax starts melting and its elasticity varies non-linearly. The rheology results presented in Figure 2 demonstrate the viscoelastic property of the wax, which has low elastic and viscous shear moduli. The Apiezon W wax is deformed on a time scale larger than its relaxation time (0.3 sec) and, therefore, strain can be accommodated by the microscopic deformation of the wax support. Thus, the wax has room for the excess strain from the semiconductor film during its elastic relaxation.

Semiconductor film strain relaxation occurs while it is still attached to the wax, during and immediate after the thinning and removal of the InP substrate (Supporting Figure S7). During the strain relaxation the wax deforms microscopically due to its viscoelastic properties in order to accommodate the excess of elastic energy supplied by the $In_xGa_{1-x}As$ film (~3.4 meV/atom), which is now in a relaxed configuration (Supporting Figure S4). The foregoing clearly support the idea that the critical feature for wafer-scale semiconductor film strain relaxation and template formation is the use of an intermediate support that has a low elastic shear modulus (5.8×10^{-7} GPa for the Apiezon wax) and, therefore, can microscopically deform to relieve the external stress applied by the strained 40 nm thick $In_xGa_{1-x}As$ film (shear modulus ~24–27 GPa for $0.36 \leq x \leq 0.58$), which is significantly more stiff.

The structural properties of the crystalline templates were determined by ω–2θ scans and reciprocal space map X-ray diffraction measurements, which give information about the lattice parameter of the film at different strain configurations. **Figure 3**a shows (004) ω–2θ scans for all samples before and after film transfer to a SiO_2/Si handling support. In all cases, the distance between the InP (sharp peak) and the 40 nm thick film (broad peak) confirms that the $In_xGa_{1-x}As$ is originally coherently-strained with respect to the substrate. After transfer, a significant peak shift is observed, resulting from strain relief (Supporting Figures S5-6). The width of the $In_xGa_{1-x}As$ peaks and the fringes confirm that the overall thickness of the film is preserved upon substrate removal. Figure 3b shows reciprocal space maps for the coherently-strained $In_xGa_{1-x}As$ on InP, taken near the asymmetric (224) reflection. The intense red peak in Figure 3b corresponds to the substrate and appears in the same position for all samples. The strained layers appear shifted in both ω and 2θ directions. The position of the film peak is used to infer the original in-plane strain values, as well as strained $a_{//}$ and $a_{\perp}$ for all samples. After the film is transferred to a Si handle wafer, a significant peak shift occurs in both ω and 2θ directions, as illustrated by the reciprocal space maps of Figure 3c.

By using the reciprocal space maps shown in Figure 3b,c, the strained and relaxed lattice parameters were quantified (Supporting Figures S8-9). For all samples strained $a_{//}$ is equal to a_{InP}, as a result of coherent epitaxial growth. To compensate the in-plane distortion of the $In_xGa_{1-x}As$ lattice-mismatched to InP, the material unit cell also deforms in the out-of-plane direction (**Figure 4**). After strain relief, the unit cells of the fabricated epitaxial templates were reconstructed. Very good agreement is found between relaxed ($a_{//}$, $a_{\perp}$) and the films natural lattice parameter, as illustrated in Figure 4. According to Vegard's Law, the material natural lattice parameter a_{film} is given by the average of the lattice parameter of the elements constituting the alloy, compensated by the molar fraction of each species. For example, a film composed of A_xB_{1-x} has a relaxed lattice parameter of $a_x = x \cdot a_A + (1-x) \cdot a_B$.[29] The content of each element will dictate a_x of the alloy and the difference between $a_{//}$ and a_{film} will determine the strain state of the film. These results demonstrate that full elastic relaxation is achieved for all samples, independent of its original strain configuration.

Figure 5 shows the room temperature, steady-state photoluminescence (PL) observed from coherent $In_xGa_{1-x}As$ films grown on InP and the corresponding relaxed $In_xGa_{1-x}As$ films after transfer to SiO_2/Si. The readily observable photoluminescence signal of the 40 nm $In_xGa_{1-x}As$ layers at room temperature confirmed the high quality of the films. Lattice-matched $In_{0.53}Ga_{0.47}As$ films on InP showed nearly identical band edge photoluminescence intensities after transfer to SiO_2/Si, demonstrating that the optoelectronic properties of the film are preserved throughout the layer transfer process (Figure 5a). Tensile-strained $In_{0.43}Ga_{0.57}As$ films on InP exhibited a significant blue shift of the PL features upon transfer to SiO_2/Si consistent with the strain relaxation observed in Figure 4. Figure 5b presents the fitting results from the low-energy portion of the PL signal using:[30]

$$I(E) = A \exp\left(\frac{E - E_g}{\alpha}\right) \tag{2}$$

where A is a proportionality constant, E_g is the bandgap, and α is a tail fit parameter. Both coherently-grown and transferred $In_{0.53}Ga_{0.47}As$ films show values of E_g and α comparable to the expected bulk parameters.[31] The tensile-strained $In_{0.43}Ga_{0.57}As$ film on InP have a similar bandgap to

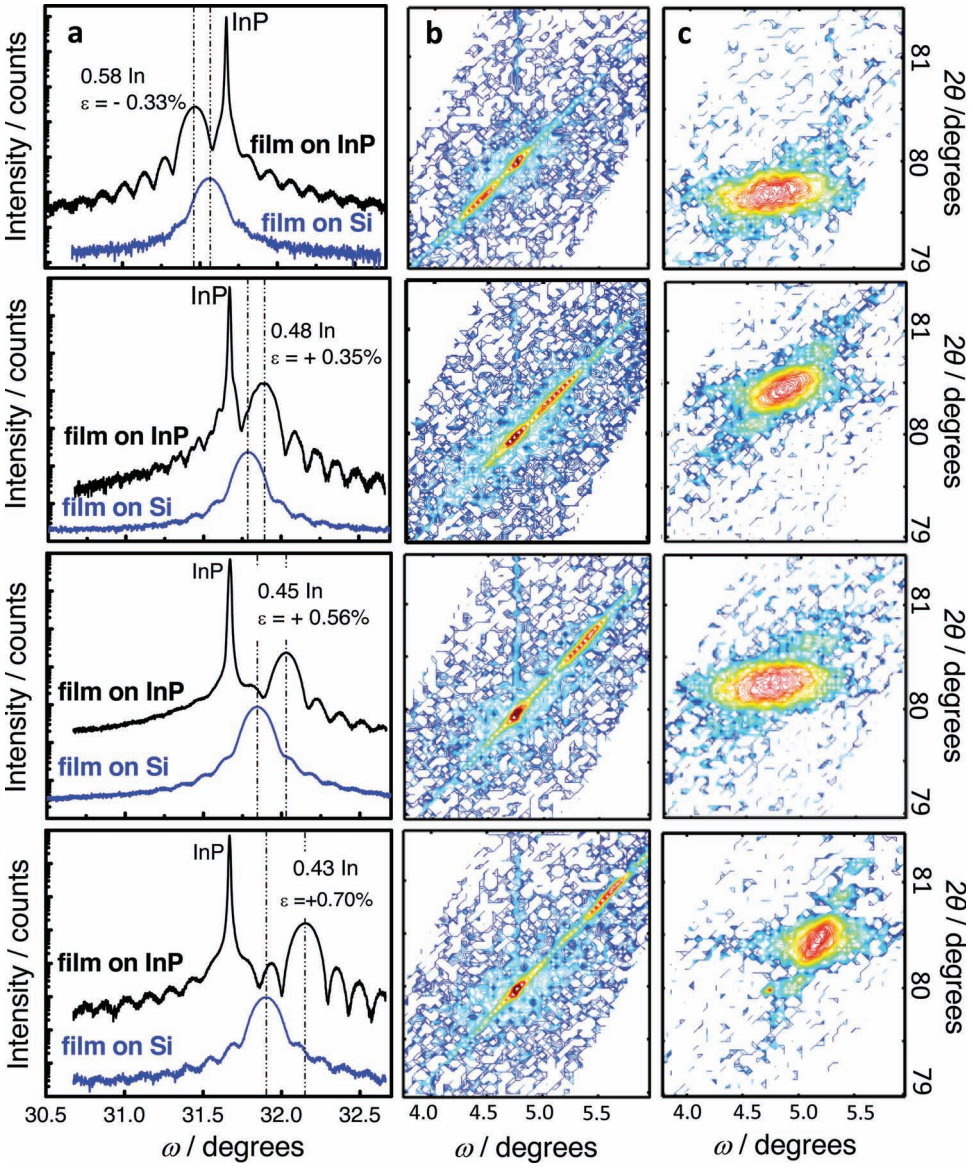

Figure 3. Structural characterization of epitaxial templates by X-ray diffraction measurements. (a) Left column: ω–2θ (004) scans of $In_xGa_{1-x}As$ films on InP substrate (black) and SiO_2/Si holder wafer (blue). The observed peak shift for all samples is due to material full relaxation. (b) Center column: Reciprocal space maps for all samples before substrate removal showing that the 40 nm thick $In_xGa_{1-x}As$:InP film is coherently-strained in all cases. (c) Right column: Reciprocal space maps after $In_xGa_{1-x}As$ films transfer to a SiO_2/Si handling support. The crystalline layer lattice parameter and film relaxation can be calculated from measurements in (c). The color scale in (b) and (c) refers to the diffracted intensity.

the $In_{0.53}Ga_{0.47}As$ films but exhibit reduced $\alpha = 4.9 \pm 0.2$, in addition to an asymmetric peak shape, consistent with the expected splitting of the heavy- and light-hole valence bands,[32] caused by the biaxial crystal distortion (Figure 4a, inset). The bandgap of the transferred $In_{0.43}Ga_{0.57}As$ film is E_g = 840 meV, blue-shifted by ~60 meV from the tensile-strained $In_{0.43}Ga_{0.57}As$ film. To summarize, the PL spectra of strained $In_xGa_{1-x}As$ films collected at room temperature clearly show the effects of film relaxation upon layer transfer to SiO_2/Si substrates.

Historically, the search for a method to synthesize a dislocation-free wafer-sized crystalline template has been a 'holy grail' objective in materials science for more than 20 years, because success in this endeavor enables the synthesis of a very large variety of strain-free crystals at lattice parameters other than those achievable via bulk crystal growth. The concept demonstrated here could be expanded to a large variety of materials, including II-VI and IV-IV semiconductors and ceramics. The creation of a single crystalline template has the potential to enable new crystalline material growth that can be employed as a building block for innovative optoelectronic designs for semiconductor heterostructures that requires tunable lattice parameters and band structures such as light-emitting diodes, photodetectors and semiconductor lasers,[33] with frequency

ADVANCED MATERIALS
www.advmat.de

www.MaterialsViews.com

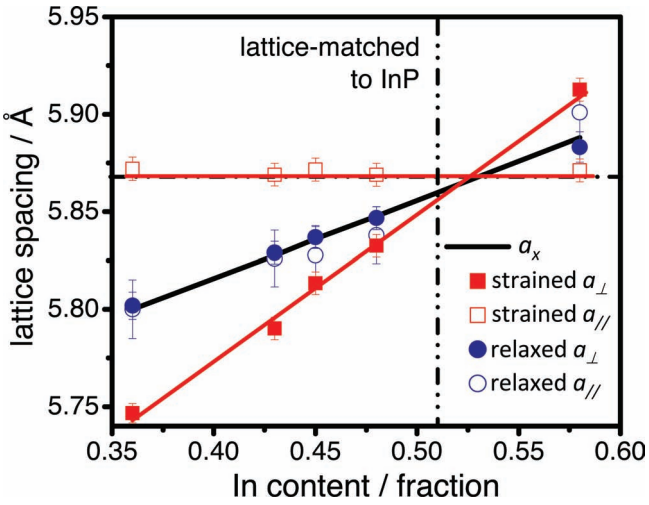

Figure 4. In-plane $a_{//}$ and out-of-plane $a_\perp$ lattice parameters for strained $In_xGa_{1-x}As$:InP films (red open and closed squares) and relaxed templates (blue open and closed circles) as a function of In content inferred from X-ray diffraction measurements of Figure 3. Full relaxation is achieved for different strain values and the data is in very good agreement with a_x predicted by Vegard's Law (black solid line). The red solid lines refer to strained $a_{//}$ and $a_\perp$ expected for coherent $In_xGa_{1-x}As$ grown on InP.

operation that are currently difficult to fabricate,[1] thin film solar cells that absorb photons with specific energies,[3] flexible electronics,[19] and woodpile-structure three-dimensional photonic crystals.[8]

Experimental Section

Templates fabrication: The templates are fabricated by epitaxial growth of 40 nm thick $In_xGa_{1-x}As$ films on InP substrates by metalorganic chemical vapor deposition at 550 °C and 3 Å/min growth rate. These conditions correspond to a kinetically controlled epitaxial growth regime, resulting in dislocation-free films. Four samples with different In content (x) were grown with distinct in-plane strain values ($\varepsilon_{//} = -0.33\%$, $+0.35\%$, $+0.70\%$, $+1.17\%$), corresponding to compressive and tensile films. The strained $In_xGa_{1-x}As$ film is initially coated with commercially available Apiezon W wax, which is dissolved in trichlotoethylene (TCE) and applied in solution. Many layers of the wax are applied to the sample surface to create in aggregate a 2 mm thick wax layer. The wax is then cured at 100 °C for 90 min and a glass slide supports the wax for handling purposes. The InP substrate is selectively etched at 5 µm/min using room temperature concentrated HCl.[34] The strain relaxation occurs when the substrate is completely removed; the $In_xGa_{1-x}As$ crystal assumes its bulk value. Once the substrate is removed the thin film is rinsed in DI H_2O and immediately placed into contact with the host substrate, e.g. SiO_2/Si. Van der Waals bonding takes place between the $In_xGa_{1-x}As$ and the handling substrate,[24] and after 24 hours the two materials are completely bonded (see Figure S3). The wax is under tension with respect to the film - ideal for layer relaxation independent of the original film strain configuration. The wax is then removed by TCE. After appropriate cleaning procedure the elastically-relaxed single crystal film is ready (Supporting Figures S1,2).

Templates characterization: The crystal quality of the single crystalline layers were inspected by transmission electron microscopy measurements using a TF30UT, a FEI Tecnai Field Emission 300 kV TEM with an ultra twin objective lens and 0.17 nm of resolution.

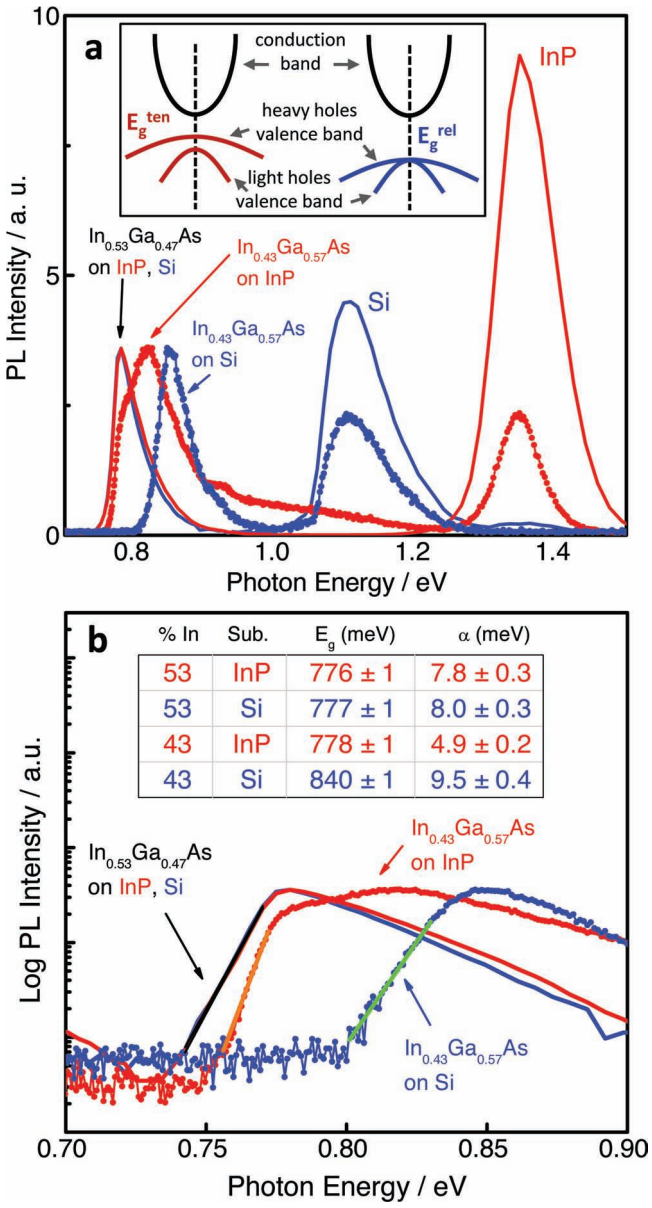

Figure 5. (a) Room temperature photoluminescence (PL) measurements of $In_{0.43}Ga_{0.57}As$ films on InP (tensile) and on Si (relaxed) and of a lattice-matched $In_{0.53}Ga_{0.47}As$ film on InP and Si. The crystal lattice distortion on the tensile $In_{0.43}Ga_{0.57}As$ film splits the valence band degeneracy. Therefore, the bandgap of a tensile film (E_g^{ten}) is smaller than the bandgap of a relaxed film (E_g^{rel}). Because the $In_{0.53}Ga_{0.47}As$ film is lattice-matched to InP no peak shift is observed. Inset: scheme of the light- and heavy-hole valence bands splitting caused by tensile strain. (b) Zoom-in of measurements in (a) with fits (solid black, orange and green lines) for the low energy portion of the spectrum (temperature independent) used to estimate E_g for each strain configuration (values are shown in the table).

X-ray diffraction measurements were performed using a conventional Cu Kα source (λ = 1.5406 Å and receiving slit = 1/2°). In order to quantify the strain relaxation, reciprocal space maps were measured.[35] Symmetric (004) and asymmetric (224) reflections were chosen for providing sufficient intensity and peak separation for zinc-blend crystal structures. The reciprocal space geometry was of glancing incidence

scans, performed to reconstruct the material unit cell. Both $In_xGa_{1-x}As$ in- and out-of-plane lattice spacings ($a_{//}$ and $a_{\perp}$) can be calculated for a certain (*h k l*) Bragg condition (see Supporting information). Knowing $a_{\perp}$, $a_{//}$ and a_x as predicted by Vegard's Law, the in-plane strain ε can be inferred as $\varepsilon = (a_{//} - a_x)/a_x$. Thus, by combining reciprocal space maps at (004) and (224) reflections, we were able to calculate the initial strain value for all samples and to quantitatively determine the strain relaxation that occurred on the $In_xGa_{1-x}As$ single crystalline layers.

For steady-state photoluminescence measurements, excitation was performed using the 488 nm line of an Ar-ion laser that was chopped at 10 kHz using an acousto-optic modulator. The emission was passed through a monochromator and focused onto an infrared photomultiplier tube, and the photoluminescence signal was monitored using a lock-in amplifier.

Supporting Information

Supporting Information is available from the Wiley Online Library or from the author. The Supporting Information contains detailed information about the epitaxial template fabrication and the characterization measurements.

Acknowledgements

The authors acknowledge J. Kornfield, J. N. Munday, and the US Department of Energy Solar Energy Technologies Program under grant DE-FG36-08GO18071 for financial support. This work benefited from use of the Caltech Materials Science TEM facility which is partially supported by the MRSEC Program of the National Science Foundation under Award Number DMR-0520565. The authors gratefully acknowledge critical support and infrastructure provided for this work by the Kavli Nanoscience Institute at Caltech. Rheology measurements were performed at the UCSB MRL Central Facilities supported by the MRSEC Program of the National Science Foundation under award No. DMR05-20415. The authors have a non-provisional patent related to this work.

Received: April 7, 2011
Revised: June 10, 2011
Published online: July 19, 2011

[1] E. F. Schubert, J. K. Kim, *Science* **2005**, *308*, 1274.
[2] F. Capasso, *Science* **1987**, *235*, 172.
[3] J. Yoon, S. Jo, I. S. Chun, I. Jung, H. S. Kim, M. Meitl, E. Menard, X. L. Li, J. J. Coleman, U. Paik, J. A. Rogers, *Nature* **2010**, *465*, 329.
[4] P. Kidd, D. J. Dunstan, H. G. Colson, M. A. Lourenco, A. Sacedon, F. GonzalezSanz, L. Gonzalez, Y. Gonzalez, R. Garcia, D. Gonzalez, F. J. Pacheco, P. J. Goodhew, *J. Cryst. Growth* **1996**, *169*, 649.
[5] Y. J. Mii, Y. H. Xie, E. A. Fitzgerald, D. Monroe, F. A. Thiel, B. E. Weir, L. C. Feldman, *Appl. Phys. Lett.* **1991**, *59*, 1611.
[6] N. J. Quitoriano, E. A. Fitzgerald, *J. Appl. Phys.* **2007**, *102*.
[7] J. Tersoff, *Appl. Phys. Lett.* **1993**, *62*, 693.
[8] S. Noda, K. Tomoda, N. Yamamoto, A. Chutinan, *Science* **2000**, *289*, 604.
[9] F. E. Ejeckam, M. L. Seaford, Y. H. Lo, H. Q. Hou, B. E. Hammons, *Appl. Phys. Lett.* **1997**, *71*, 776.
[10] K. D. Hobart, F. J. Kub, M. Fatemi, M. E. Twigg, P. E. Thompson, T. S. Kuan, C. K. Inoki, *J. Electron. Mater.* **2000**, *29*, 897.
[11] H. Yin, K. D. Hobart, F. J. Kub, S. R. Shien, T. S. Duffy, J. C. Sturm, *Appl. Phys. Lett.* **2003**, *82*, 3853.
[12] J. F. Damlencourt, J. L. Leclercq, M. Gendry, M. Garrigues, N. Aberkane, G. Hollinger, *Jpn. J. Appl. Phys. Part 2 - Lett.* **1999**, *38*, L996.
[13] J. F. Damlencourt, J. L. Leclercq, M. Gendry, P. Regreny, G. Hollinger, *Appl. Phys. Lett.* **1999**, *75*, 3638.
[14] M. Boudaa, P. Regreny, J. L. Leclercq, M. P. Besland, O. Marty, G. Hollinger, *J. Electron. Mater.* **2004**, *33*, 833.
[15] H. Fang, M. Madsen, C. Carraro, K. Takei, H. Sul Kim, E. Plis, S.-Y. Chen, S. Krishna, Y.-L. Chueh, R. Maboudian, A. Javey, *Appl. Phys. Lett.* **2011**, *98*, 012111.
[16] M. M. Roberts, L. J. Klein, D. E. Savage, K. A. Slinker, M. Friesen, G. Celler, M. A. Eriksson, M. G. Lagally, *Nat. Mater.* **2006**, *5*, 388.
[17] F. Cavallo, M. G. Lagally, *Soft Matter* **2010**, *6*, 439.
[18] C. Euaruksakul, Z. W. Li, F. Zheng, F. J. Himpsel, C. S. Ritz, B. Tanto, D. E. Savage, X. S. Liu, M. G. Lagally, *Phys. Rev. Lett.* **2008**, *101*.
[19] D. Y. Khang, H. Q. Jiang, Y. Huang, J. A. Rogers, *Science* **2006**, *311*, 208.
[20] H. Fang, M. Madsen, C. Carraro, K. Takei, H. S. Kim, E. Plis, S.-Y. Chen, S. Krishna, Y.-L. Chueh, R. Maboudian, A. Javey, *Appl. Phys. Lett.* **2011**, *98*, 012111.
[21] H. Ko, K. Takei, R. Kapadia, S. Chuang, H. Fang, P. W. Leu, K. Ganapathi, E. Plis, H. S. Kim, S.-Y. Chen, M. Madsen, A. C. Ford, Y.-L. Chueh, S. Krishna, S. Salahuddin, A. Javey, *Nature* **2010**, *468*, 286.
[22] K. Lee, K.-T. Shiu, J. D. Zimmerman, C. K. Renshaw, S. R. Forrest, *Appl. Phys. Lett.* **2010**, *97*, 101107.
[23] E. Yablonovitch, T. J. Gmitter, J. P. Harbison, R. Bhat, *Appl. Phys. Lett.* **1987**, *51*, 2222.
[24] E. Yablonovitch, D. M. Hwang, T. J. Gmitter, L. T. Florez, J. P. Harbison, *Appl. Phys. Lett.* **1990**, *56*, 2419.
[25] J. F. Klem, E. D. Jones, D. R. Myers, J. A. Lott, *J. Appl. Phys.* **1989**, *66*, 459.
[26] N. Lucas, H. Zabel, H. Morkoc, H. Unlu, *Appl. Phys. Lett.* **1988**, *52*, 2117.
[27] J. Bak-Misiuk, J. Wolf, U. Pietsch, *Phys. Stat. Sol.* **1990**, *118*, 209.
[28] R. B. Bird, W. E. Stewart, E. N. Lightfoot, *Transport Phenomena*, John Wiley & Sons Inc., Second ed., NY, USA **2007**.
[29] J. Y. Tsao, *Materials Fundamentals of Molecular Beam Epitaxy* London **1993**.
[30] R. K. Willardson, A. C. Bebb, *Semiconductors and Semimetals*, Vol. *8*, Academic Press Inc, NY, USA **1972**.
[31] I. C. Bassignana, C. J. Miner, N. Puetz, *J. Appl. Phys.* **1989**, *65*, 4299.
[32] C. P. Kuo, S. K. Vong, R. M. Cohen, G. B. Stringfellow, *J. Appl. Phys.* **1985**, *57*, 5428.
[33] S. Mokkapati, C. Jagadish, *Mater. Today* **2009**, *12*, 22.
[34] A. R. Clawson, *Mater. Sci. Eng. R-Rep.* **2001**, *31*, 1.
[35] P. v. d. Sluis, *J. Phys. D: Appl. Phys.* **1993**, *26*, A188.